



Carbonation resistance of fly ash and blast furnace slag based geopolymer concrete

Zhuguo LI^{a,*}, Sha LI^b

^a Graduate School of Science and Technology for Innovation, Yamaguchi University, Ube 755-8611, Japan

^b Graduate School of Science and Engineering, Yamaguchi University, Ube 755-8611, Japan

HIGHLIGHTS

- The carbonation resistance of fly ash (FA) & blast furnace slag (BFS)-based geopolymer (GP) concrete were investigated in detail by theoretical analysis and the accelerated carbonation test.
- Carbonation rates of the ambient cured GP concrete and GP mortar were modeled by power functions.
- The influencing factors of carbonation rate of GP concrete were clarified, including retarder addition, BFS's ratio and fineness, NaOH content, and curing temperature, etc.
- The relationship between carbonation resistance and compressive strength of GP concrete was discussed.

ARTICLE INFO

Article history:

Received 22 September 2017

Received in revised form 15 December 2017

Accepted 17 December 2017

Keywords:

GP concrete

Carbonation resistance

Carbonation rate model

Fly ash

Blast furnace slag

ABSTRACT

For putting geopolymer (GP) to practical use in reinforced concrete, the carbonation resistance of GP concrete should be clarified. In this study, the carbonation depths of various GP concrete and GP mortar, of which the aluminosilicate materials were fly ash (FA) and ground blast furnace slag (BFS), were measured by the accelerated carbonation test at different elapsed times. The relationship between the carbonation depth and the elapsed time were further examined based on the experimental results and by theoretical analysis. A root function was proposed to describe the carbonation rate of FA&BFS-based GP concrete. Finally, the influencing factors of carbonation resistance of FA&BFS-based GP concrete were discussed through a comparison of carbonation rate coefficients. It is mainly concluded that the carbonation resistance of FA&BFS-based GP concrete cured at room temperature is lower than usual concrete using Ordinary Portland Cement (OPC). The carbonation resistance increases with the increase of BFS ratio in active fillers (AF), NaOH content in active activator solution (AS), and BFS fineness, or with the decrease of AS/AF ratio, and water/AF ratio. Moreover, heat curing and the use of the retarder are benefit to the carbonation resistance of FA&BFS-based GP concrete.

© 2017 Elsevier Ltd. All rights reserved.

1. Introduction

Ordinary Portland Cement (OPC) is produced along with much energy consumption and limestone decomposition. Cement industry emits so much CO₂ that accounts for 5–7% of national CO₂ emission [1,2]. Geopolymer (GP) is a type of inorganic polymer that can make from industrial waste or by-product, and can harden even at room temperature so that it would function as a binder in concrete like OPC. GP has been proved to be advantage over OPC concrete in early strength growth, and in the resistances to fire and aggressive

chemicals [3–6], thus it is considered as a potential alternative to OPC.

The most readily available source materials of GP are fly ash (FA) and ground granulated blast furnace slag (BFS), which are aluminosilicate minerals composed of aluminum, silicon, and oxygen, etc. FA-based geopolymer can cut down about 60% CO₂ emission, compared to OPC [7]. However, in order to improve the strength of FA-based geopolymer cured at room temperature, BFS has to generally be blended. In addition, alkali-activated slag is also thought to be an alternative to OPC.

There are many investigations on the three kinds of alkali-activated materials-FA, BFS, and FA&BFS-based GP concrete. But these investigations are mainly focused on recipes, mechanical properties, and reaction products. However, for putting GP to

* Corresponding author.

E-mail address: li@yamaguchi-u.ac.jp (Z. LI).

practical use in reinforced concrete, detailed investigation of GP concrete's durability, especially carbonation resistance, is very necessary [8].

Adam, et al. [9] compared the carbonation resistances of FA-based GP concrete cured at 80 °C, BFS-based GP concrete, and BFS-OPC blended concrete by the accelerated carbonation test in the ambient air of 20 °C, 70% R.H., and 20% of CO₂ concentration. The latter two concretes were cured at room temperature. They found that the FA-based GP concrete didn't show a clear boundary between the carbonated and non-carbonated area after sprayed the phenolphthalein solution. Also, it was found that BFS-based GP concrete has a lower carbonation resistance than FA-based GP and OPC-BFS blended concretes since BFS-based GP concrete specimen had more inside micro-cracks, and its C–S–H gel has in general a lower Ca/Si ratio than the C–S–H in OPC concrete. The C–S–H gel with low Ca/Si ratio is thought to carbonate faster than the general C–S–H gel. Adam, et al. [10] also measured the pH changes of FA-based GP mortars, which were mixed with different alkali activators, during accelerated carbonation under 20 °C, 70% R.H., and 5% of CO₂ concentration. The pH values of the GP mortars fell from 12 to 11 after carbonated. Initial pH (=12) of GP mortar was smaller than that (pH = 13) of OPC concrete, but final pH (=11.0) was higher than OPC concrete (pH = 9.0). This results are nearly consistent with the Davidovitz's finding that pH ranges of GP concrete are 11.5–12.5, and 10.0–10.5, respectively before and after carbonation [11]. Based on this result, Adam, et al. concluded that GP concrete with the pH value of over 11, which is a safe value for preventing reinforcing steel from corrosion, would be achieved by using adequate alkali activator and aluminosilicate materials.

Song, et al. [12] investigated the carbonation resistance of BFS-based GP mortars, mixed with different amounts of alkali activator and cured in sealed state, by measuring their carbonation depths and the micro-structures before and after carbonated. They found that before carbonation, there were C–S–H gel and few aluminum compounds but no portlandite (Ca(OH)₂) in the BFS-based GP mortars. However, the C–S–H gel is more vulnerable to CO₂ than that in OPC paste. After carbonation, the C–S–H gel changed to silica gel, and the aluminum compounds completely disintegrated. Thus, the carbonation resistance of BFS-based GP is lower than that of OPC. However, they suggested that as the alkali activator content increased, the carbonation resistance of BFS-based GP was improved.

Bernal, et al. [13] detected and compared the changes in the nano-structures of BFS-based GP, FA-based GP, and FA&BFS-based GP before and after carbonation in detail. It was found that N–A–S–H is a main product in FA-based GP and almost can't be disintegrated by carbonation, and only the alkali activator in the pores is neutralized by CO₂. However, once BFS is blended in GP, the C–A–S–H gel is also formed. The C–A–S–H gel would be decalcified in CO₂ environment to cause the structural transformation at a relatively greater degree.

Criado, et al. [14] examined the effect of curing condition on the early carbonation, and concluded that heat curing with surface sealing can prevent the early carbonation and make the alkali activated FA paste to reach a high degree of polycondensation reaction. The reaction degree affects GP paste's strength and carbonation resistance.

Pasupathy, et al. [15] investigated continuously the carbonation degrees of two kinds of FA&BFS-based GP concretes in the air for 8 years. On basis of supposing that the carbonation depth of GP concrete is a root function of elapsed time (*t*, year) as $x = K\sqrt{t}$, the authors concluded that the carbonation rate coefficient *K* (mm/√year) is positively correlated to the permeability, porosity, and pore size of GP concrete. They also found that the GP concrete, only using NaOH or KOH solution as alkali activator, had a greater car-

bonation resistance than that using NaOH or KOH together with sodium silicate.

In summary, up to now, 1) there are still few studies on the carbonation resistance of GP concrete, 2) most of studies are for the GP concretes cured at elevated temperature, 3) influencing factors of carbonation resistance were not yet clarified, and 4) there is no carbonation rate model to predict the carbonation depth of GP concrete at any age. However, the carbonation rate of concrete correlates closely with the service life of reinforced concrete.

In fact, if curing in the ambient air, FA-based GP concrete sets slowly, and has a small ultimate strength [16]. In order to attain a practical compressive strength, BFS is generally mixed together with FA. With the mix of BFS, the setting time becomes short but the strength increases [16,17]. The similar results were observed in our experiments [18]. Even if FA & BFS-based concrete has practical strength, too short setting time or handling time less than one hour would result in a difficulty of practical use in construction site. Li, et al. successfully developed a retarding admixture for FA&BFS-based GP concrete [19]. The retarder can prolong the setting time of FA&BFS-based GP concrete by 1.5–2.3 times, together with almost not giving bad effect on the compressive strength. However, the carbonation resistance of FA&BFS-based GP concrete using retarder has not yet been investigated.

FA&BFS-based GP concrete not only can recycle much waste discharged from thermal power station, but also it has a practical strength even though cured in the ambient air. In order to clarify the carbonation resistance of FA&BFS-based GP concrete, in this study we first investigated the carbonation depths of FA&BFS-based GP concretes and mortars by the accelerated carbonation test. Then a carbonation rate model was proposed to describe the relationship between the carbonation depth and the elapsed time. Furthermore, the influencing factors of the carbonation rate of FA&BFS-based GP concrete were discussed, including alkali activator content, replacing ratio of BFS, alkali activator sort, fineness of BFS, retarder, ratio of alkali activator to active filler, curing temperature, and compressive strength, etc.

2. Experimental program

2.1. Raw materials used

Besides the fly ash that met the quality standard of JIS (Japanese Industrial Standards) fly ash grade II, three kinds of BFS with different fineness were used as active filler (AF) of GP concrete in this study, of which physical properties and chemical compositions are shown in Table 1. Fine aggregates used in GP concrete and GP mortar were river sand and sea sand with specific gravity of 2.60 and 2.57, respectively. Coarse aggregate used in GP concrete was crushed limestone with specific gravity of 2.70, and a maximum size of 20 mm. The specific gravity of aggregate was measured in the saturated surface-dry state. Fine and coarse aggregates were used under the saturated surface-dry condition. The retarder (R) is an inorganic compound with specific gravity of 1.78.

Four kinds of alkali activator solutions (AS), named AS₁, AS₂, AS₃ and AS₄ were used in GP concretes. They were mixtures of water glass aqueous solution (WG) and sodium hydroxide solution (NH) according to the volume ratios shown in Table 2. The WG was prepared by diluting JIS No.1 grade water glass with distilled water by a volume ratio of 1:1. The concentration of NH was 10 mol.

2.2. Mix proportions of GP concrete and mortar

In our experiments, 14 kinds of GP concretes and 9 kinds of mortars with different mix proportions, as summarized

Table 1
Physical properties and chemical compositions of active fillers.

Active Filler (AF)	Physical property		Chemical composition (%)								
	Specific gravity	Blaine fineness (cm ² /g)	SiO ₂	Al ₂ O ₃	CaO	Fe ₂ O ₃	MgO	Na ₂ O	K ₂ O	TiO ₂	Others
FA	2.24	3550	62.09	23.04	2.07	6.88	0.67	0.45	1.68	1.41	1.62
BFS30P	2.90	3200	33.82	15.11	43.64	0.28	5.67	0.26	0.25	0.56	0.41
BFS40P	2.88	4180	34.67	14.46	43.13	0.34	5.50	0.25	0.25	0.55	0.85
BFS60P	2.91	5810	34.30	14.36	43.50	0.28	5.86	0.26	0.22	0.59	0.63

Table 2
Alkali activator's components and density.

Alkali Activator	WG: NH (by volume)	Specific gravity
AS ₁	1:0	1.270
AS ₂	3:1	1.315
AS ₃	2:1	1.320
AS ₄	0:1	1.330

respectively in Tables 3 and 4, were used to investigate the carbonation resistance and its influencing factors of GP materials. The GP concrete specimens were produced in different times, differentiating with alphabet A (June 2016) and B (Oct. 2016) in the series No. In case of GP mortar, the ratio of fine aggregate (S) to active filler (AF) was around 2.0 by mass, and the alkali activator to active filler ratio was 0.5.

Criado, et al. [20] stated that the main reaction product of active fillers containing above 60% BFS is C–A–S–H gel, but when the replacing ratio of BFS is below 40%, the main product becomes to be N–A–S–H gel. Now there is no generally accepted definition about geopolymer, but it is thought that geopolymer has at least two features: three-dimensional structure and amorphousness. Since the N–A–S–H gel tends to be amorphous and a three-dimensional structure, we limited the replacing ratio of BFS to 50% in this study. Another reason is to use FA in GP concrete as much as possible by limiting the BFS content.

2.3. Specimen preparation

The experimental procedure is shown in Fig. 1. A concrete mixer with two horizontal blades and a Hobart planetary mortar mixer were used to mix GP concrete, and GP mortar, respectively. In case of concrete, active fillers and fine aggregate were firstly put into the concrete mixer and mixed for 1 min. Then, the alkali activator and retarder were added and mixed for 2 min. to get GP matrix mortar. Finally, coarse aggregate was added to the mortar and further mixed for 2 min. to get GP concrete. After the slump and air

content were measured, fresh concrete was cast half and half into the plastic cylinder molds with a diameter of 10 cm and a height of 20 cm. Every half casting accompanied 10 s of vibration using a rod vibrator. Following by the vibration, the outside of mold was tapped by a wood hammer.

The mixing procedure of GP mortar was the same to GP concrete except not adding coarse aggregate. Freshly mixed GP mortar was used to produce two kinds of specimen: cylinder with a diameter of 10 cm and a height of 20 cm, and prism with 4 cm of side length of square and 16 cm of height, respectively. The former was for the accelerated carbonation test, and the latter was used to measure the mechanical properties. 1 min. vibration was applied to each of the mortar specimens with a table vibrator. The top surfaces of all the specimens were leveled by a metal spatula.

The specimens of concrete and mortar were cured in the ambient air of 20 ± 2 °C, R.H. 60 ± 5% for 28 days except Series No.2 and No.3. GP concrete specimens were demoulded at 5 days age. However, the GP mortar specimens were demoulded at 1 day age except Series No.6 that set 2 days later.

The mortar specimens of Series No.2 and Series No.3 were cured at 60 °C, and 80 °C for 8 h, respectively, following by curing in the ambient air of 20 ± 2 °C, R.H., 60 ± 5% till 28 days age. Demoulding was done after the first 3 h curing of 60 °C or 80 °C.

The compressive strengths (f_c) of GP concretes were measured at 28 days age according to JIS A 1108, which were average values of three specimens for each series, as shown in Table 3.

2.4. Accelerated carbonation test

After the 28 days curing, the top and the base of every cylindrical specimen were sealed with waterproof tape to ensure that CO₂ diffuses into the specimens only through the circumferential surface, as shown in Fig. 2. Then, the specimens were placed into a carbonation test chamber with 5% of CO₂ concentration, 20 °C, and R.H. 60%. At an interval of one week, the concrete or mortar specimen was cut at 35–40 mm intervals to measure the

Table 3
Mix proportions and compressive strength of GP concrete.

Influencing factors	Series No.	AS (kg/m ³)	AS/AF	FA/AF	BFS/AF	BFS sort	R/AF (%)	S (kg/m ³)	G (kg/m ³)	f_c (MPa)
AS content	1A	AS ₂ =210	0.50	0.7	0.3	40P	5	721	1000	25.0
	2A	AS ₂ =200						762		28.4
	2B							762		29.7
AS/AF	3A	AS ₂ =185	0.45					824		27.4
	4B	AS ₂ =200						704		28.4
	5B							790		27.7
AS sort	6B	AS ₁ =200	0.50			30P	0	749		19.1
	7B	AS ₂ =200						752		41.8
	8B	AS ₄ =200						768		20.1
BFS content	9B	AS ₂ =200		0.5	0.5	40P	5	771		40.0
	10A							782		31.0
	11A							753		23.5
	12B							723		17.7
Retarder	13A			0.8	0.2			753		23.8

[Notes] AS: Alkali activator, AF: Active filler, FA: JIS grade II fly ash, BFS: Ground granulated blast furnace slag, R: Retarder, S: Fine aggregate, and G: Coarse aggregate, f_c : 28 days compressive strength

Table 4
Mix proportions and curing temperature of GP mortar.

Series No.	1	2	3	4	5	6	7	8	9
Curing temperature (°C)	20	60	80	20					
AS/AF	0.5								
S/AF	2.0								
AS sort	AS ₂			AS ₁	AS ₃	AS ₄	AS ₂		
R/AF (%)	5						0	5	
BFS sort	40P							30P	60P

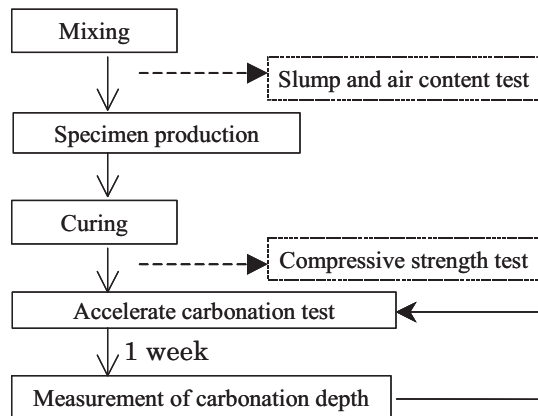


Fig. 1. Experimental procedure.

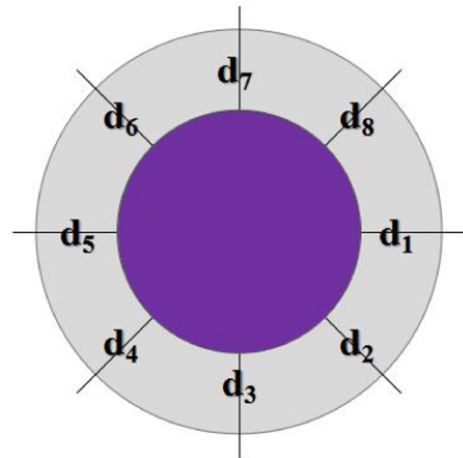


Fig. 3. Measurement positions of carbonation depth.

carbonation depth. It should be noted that during the cutting, in order to ensure that the alkali matters were not washed away, spraying water was not used as dust countermeasure.

After the measurement of carbonation depth, the specimens were returned into the CO₂ chamber to continue the carbonation test, following by sealing the cut section with the tape. The accelerated carbonation test lasted 8 weeks, and 6 weeks for concrete and mortar specimens, respectively.

The method, used to measure the carbonation depth of GP specimen in this study, is the same to that usually used for OPC concrete, i.e. spraying phenolphthalein on freshly cut section, then measuring the depths of colorless region in 8 directions on the cross section of cylindrical specimen, finally calculating average value of the 8 depths, as shown in Fig. 3.

Other researchers [21,10,22] pointed out that the interface between carbonated and non-carbonated zones of GP specimens is unstable after spraying phenolphthalein solution, we also observed that the pink color area changes with the elapsed time,



Fig. 2. Specimen's section sealed with waterproof tape.

as shown in Fig. 4. However, if the measurement is done early, it is able to distinguish the pink color boundary definitely, and measure the carbonation depth precisely. Hence, we measured the carbonation depths at 8 positions within 3–5 min. after spraying the phenolphthalein solution.

3. Test results and discussion

3.1. Pink color range on the specimen section after spraying phenolphthalein solution

Table 5 shows the color changes on the cross sections of all the specimens at 5 min. later after phenolphthalein solution was sprayed, which were carbonated for 8 weeks. Almost all of the GP concrete specimens except Series No.12B had clear pink boundary, and the pink area decreased with the carbonation time. The pink boundary was not in a cycle, interrupted by coarse aggregate particles.

Series No.12B was actually FA-based GP concrete, not using BFS so that its strength was small. That is to say, it had not a dense structure and thus was easily carbonated. Maybe Series No.12B was greatly carbonated during the curing, which resulted in that it had a pale pink area even before the accelerated carbonation test, as shown in Table 5 (continued).

3.2. Variation of carbonation depth with elapsed time

Fig. 5 shows the test results of the relationship between the carbonation depth (C-depth) and the elapsed time for the GP concretes. The carbonation depth increased with the elapsed time in the first three week, but after three week, the increase became smaller and smaller.

The relationship between the carbonation depth of GP mortar and the elapsed time are shown in Fig. 6. Like as the GP concrete,

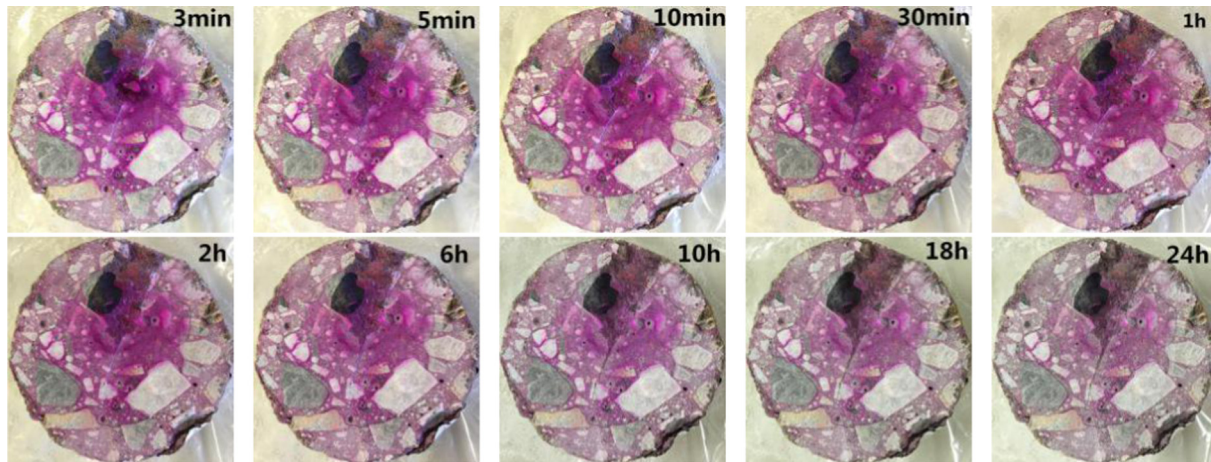


fig. 4. Color change after spraying the phenolphthalein solution.

the carbonation of GP mortar progressed rapidly with time in the first two weeks, and then evolved slowly.

3.3. Carbonation rate model

3.3.1. Theoretical analysis of carbonation rate

According to Fick's first law [23], the diffusion flux of carbon dioxide into concrete through unit cross section at unit time (Q , $\text{g}/\text{m}^2 \text{ s}$) is expressed by Eq. (1), assuming that the carbon dioxide concentration (φ) just changes with diffusing depth (x).

$$Q = -D \frac{\partial \varphi}{\partial x} \quad (1)$$

where, D is the diffusion coefficient of CO_2 (m^2/s)

The relationship between the CO_2 concentration (φ) and the diffusing depth (x) is generally simplified as a linear relationship, i.e. the φ decreases linearly with the x . If the CO_2 concentration at the surface of concrete is noted as φ_0 , Eq. (1) can be changed as Eq. (2).

$$Q = D \frac{\varphi_0}{x} \quad (2)$$

Before the CO_2 diffuses to the position x , it must be consumed or bound by the chemicals located on the diffusing route. For OPC concrete, main chemical substance reacting with CO_2 is generally $\text{Ca}(\text{OH})_2$. But for GP concrete, the chemicals are not clear. The CO_2 is perhaps bound by unconsumed alkali activator.

The diffusion flux of carbon dioxide can be expressed by Eq. (3)

$$dJ = Q \cdot S \cdot dt \quad (3)$$

where, J is the mass of chemically bound CO_2 in concrete (g), t is time (s), S is the surface through which the diffusion occurs (m^2).

If the CO_2 absorption capacity of concrete due to carbonation through a unit surface area in unit time is noted by q (g/m^3), dJ can be given by Eq. (4).

$$dJ = q \cdot S \cdot dx \quad (4)$$

For the materials that do not react with diffusing gas, e.g. sand and soil, their gas diffusion coefficients are constant, not changing with the exposed time. However, for hardened concrete, it is generally considered that the carbonation products, such as CaCO_3 in case of OPC concrete, make concrete dense so that the porosity decreases since the volume of CaCO_3 is larger than that of $\text{Ca}(\text{OH})_2$ by about 11.7% [24,25]. Yang's model [26] shows that the diffusion coefficient of OPC concrete is directly proportional to the square of porosity, and decreases with the advance of hydration and carbonation.

Fig. 7 shows the SEM images of GP mortar before and after the carbonation. It can be found that after carbonation, the fine cracks disappeared and the coarse cracks became small, i.e. the GP concrete became dense. Moreover, the compressive strengths of Series No.2B were 29.7 MPa, and 34.2 MPa before and after the carbonation, respectively. The increase of strength also indicates that the GP concrete became dense after the carbonation. Therefore, we consider that the diffusion coefficient (D) of GP concrete would decrease with the carbonation time (t) as OPC concrete.

Czarnecki [27] investigated the relationship between the diffusion coefficient (D) and t for OPC concrete, and proposed a D - t relationship model, as shown in Eq. (5). The diffusion coefficient of OPC concrete decreases with the elapsed time. It is generally considered that this is because the CaCO_3 fills up the pores in concrete.

$$D = 28.085t^{-0.439} \quad (5)$$

It is not easy to examine how the diffusion coefficient of GP concrete changes with carbonation time. In this study, we firstly supposed that Eq. (5) is also applied to FA&BFS-based GP concrete since the carbonation constituent (e.g. NaOH) in GP concrete reacts with CO_2 to form Na_2CO_3 like the generation of CaCO_3 in OPC concrete.







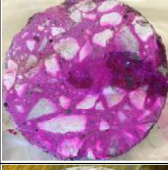
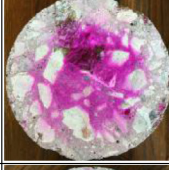











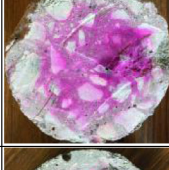


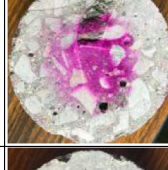



















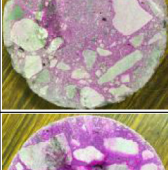

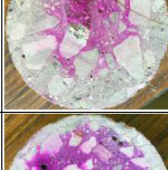

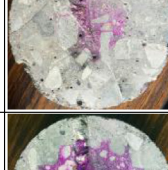
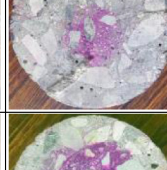





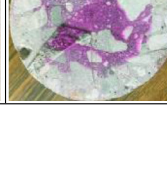
The amount of $\text{Ca}(\text{OH})_2$, which is a kind of hydrates, depends on hydration degree of cement. $\text{Ca}(\text{OH})_2$ is also main carbonation constituent of OPC concrete. Thus, for a certain OPC concrete, the CO_2 absorption capacity increases with the age of concrete, as shown in Eq. (6) [26].

$$q = \frac{8.06t_c}{2.0 + t_c} \alpha_\infty \cdot C \cdot M_{\text{CO}_2} \quad (6)$$

where t_c is the age of concrete, α_∞ is the ultimate degree of hydration, C : cement content in 1 m^3 concrete, and M_{CO_2} is the molecular weight of CO_2 (44 g/mol.)

Now the carbonation mechanism of GP concrete is not fully clear. Remained alkali activator, C-A-S-H gel, and N-A-S-H gel are possible to react with CO_2 . As the C-A-S-H and N-A-S-H gels form, the alkali activator decreases. Hence, we can't conclude that whether the CO_2 absorption capacity of GP concrete increases with carbonation time or not. However, according to the Eq. (6), for a given OPC concrete (C is constant), the increase of the CO_2 absorption capacity with time is not great. Also, unless GP concrete is kept in moist state by sealing, its long-term strength growth is very small. Therefore, in this study we ignored the change of the CO_2 absorption capacity of GP concrete, i.e. treated the q as a constant for a given GP concrete.

Table 5
Pink color ranges of concrete specimens before and after the accelerated carbonation.

No.	Before	1 week	2 weeks	4 weeks	6 weeks	8 weeks
1A						
2A						
2B						
3A						
4B						
5B						
6B						
7B						
8B						

(continued on next page)

Table 5 (continued)

No.	Before	1 week	2 weeks	4 weeks	6 weeks	8 weeks
9B						
10A						
11A						
12B						
13A						

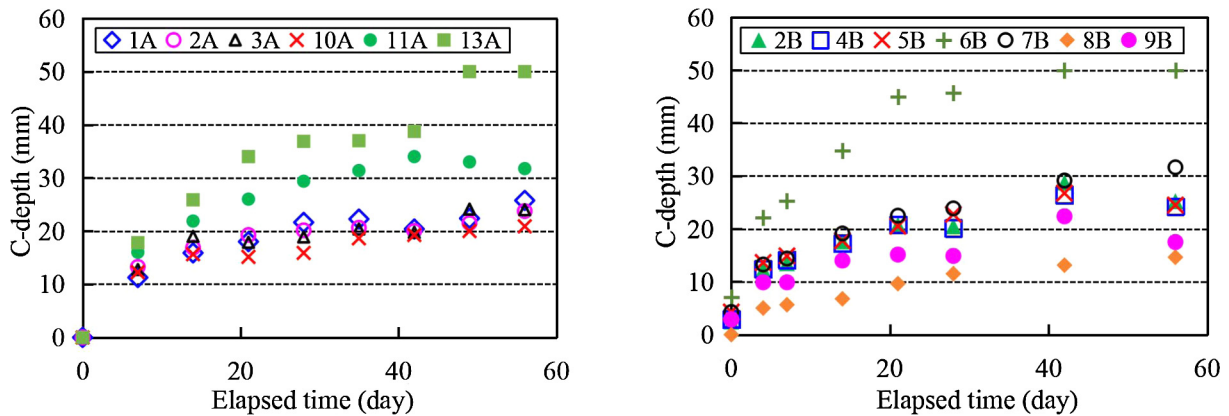


Fig. 5. Relationship between the carbonation depth of GP concrete and the elapsed time.

Eqs. (4) and (5) were substituted into Eqs. (2) and (3) respectively, and based on the consideration that the CO₂ diffusion amount is equal to the CO₂ absorption amount, Eq. (7) was obtained as follows.

$$x dx = \frac{28.085 \cdot \varphi_0}{q} t^{-0.439} dt \tag{7}$$

$$q \frac{dx}{dt} = 28.085 \cdot t^{-0.439} \cdot \frac{\varphi_0}{x}$$

Furthermore, after integrating the two sides of Eq. (7) with respect to the depth x , and the elapsed time t , respectively, the relational equation of carbonation depth and time was gotten, as shown in Eq. (8).

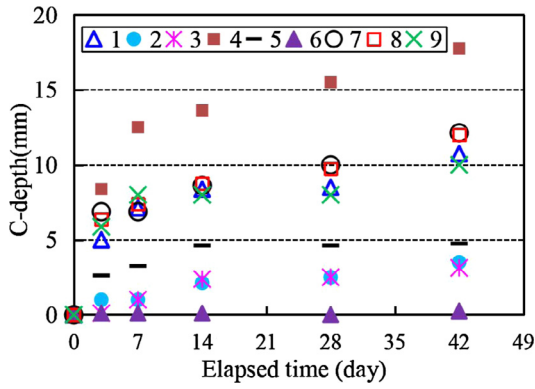


Fig. 6. Relationship between the carbonation depth of GP mortar and the elapsed time.

$$x = 10 \sqrt{\frac{\phi_0}{q}} \cdot t^{0.28} \tag{8}$$

The carbonation depth-time relational equation Eq. (8) was simplified as Eq. (9). The parameter a is defined to be the carbonation rate coefficient of GP concrete. From Eq. (9), we can understand that the carbonation rate of GP concrete in the early time of carbonation is greater than in the long time. Also, the carbonation depth of OPC concrete is generally thought to be the square root function of carbonation time. Hence, the increasing rate of carbonation depth of GP concrete is larger than that of OPC concrete in the early time of carbonation. When FA&BFS-based GP concrete cured in the ambient air has the same 28-days compressive strength to OPC concrete, the carbonation rate coefficient of the former, which is also a proportional coefficient of square root function like as OPC concrete, is larger than that of the latter [28].

$$x = a \cdot t^{0.28} \tag{9}$$

3.3.2. Experimental analysis of carbonation rate

Since the above theoretical analysis was performed on basis of several suppositions, Eq. (9) should be verified by experimental results. Next, we further conducted regression analyses toward the experimental results shown in Fig. 5, according to root function shown in Eq. (10). Several n values of root equation were used in

the regression analyses, which were around 0.28 besides 0.5 according to Eq. (9).

$$x = at^{1/n} \tag{10}$$

where, x means carbonation depth (mm), t represents carbonation time (day), a is proportional coefficient, i.e. carbonation rate coefficient, and n is a positive number.

The proportional coefficients (a) of six kinds of root functions ($1/n = 0.50, 0.33, 0.35, 0.30, 0.28, 0.25$), and the determination coefficients (R^2) were obtained from the regressive curve equations of GP concrete, as shown in Table 6. The standard deviation (σ) of R^2 was gotten for every series (see Table 6). The R^2 and the σ changed with the $1/n$ used. The greater the R^2 and the smaller the σ , the higher the accuracy of the regressive equation.

For getting a root function that is universally applied to describe the carbonation evolution of FA&BFS-based GP concrete cured in the ambient air, we plotted the relationships of R^2 , σ and $1/n$, as shown in Fig. 8(a). From Fig. 8(a), we found that with the increase of $1/n$, the R^2 increases and the σ decreases, but beyond a certain value of $1/n$, the R^2 starts to decrease and the σ starts to increase. When $1/n$ is in a range of 0.28–0.33, both the R^2 and the σ reached each satisfactory value.

In order to get an optimum value of $1/n$ for the root function, the regressive analyses were conducted for the relationships between the R^2 , the σ and the $1/n$ to get two relational equations, as shown in Eqs. (11) and (12). The determination coefficients of the two equations are larger than 0.99. This indicates that the accuracy of regressive curve equation of carbonation depth is greatly dependent on the $1/n$ value.

$$R^2 = -2.531(1/n)^2 + 1.5804(1/n) + 0.6975, \text{ Determination coefficient} : 0.9998 \tag{11}$$

$$\sigma = 1.312(1/n)^2 - 0.8285(1/n) + 0.1551, \text{ Determination coefficient} : 0.9975 \tag{12}$$

Through a maximum-minimum problem analysis, we found that for achieving a maximum R^2 , $1/n$ should be 0.3122, and for getting a minimum σ , the $1/n$ should be 0.3157. Hence, the optimum value of $1/n$ is about 0.31.

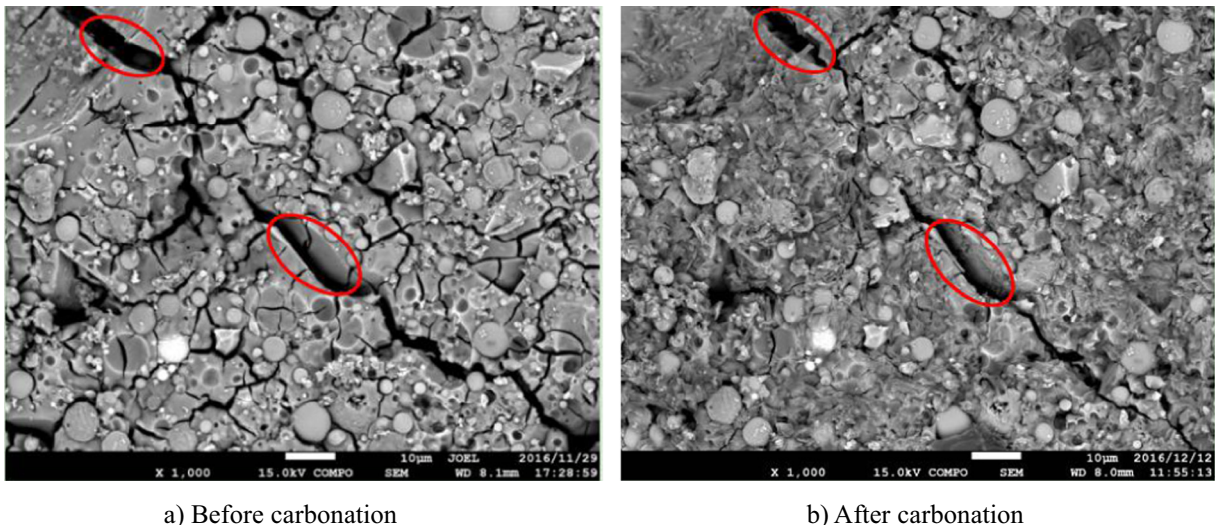


Fig. 7. The SEM images of series No.1 before and after carbonation.

Table 6
The carbonation rate coefficient of FA&BFS-based GP concrete.

No.	Carbonation rate coefficient a						Determination coefficient R^2					
	$1/n$						$1/n$					
	1/4	0.28	0.30	1/3	0.35	1/2	1/4	0.28	0.30	1/3	0.35	1/2
1A	8.6439	7.7678	7.2721	6.4726	6.1042	3.5678	0.9575	0.9664	0.9697	0.9721	0.9716	0.9253
2A	8.4519	7.5879	7.0995	6.3125	5.9503	3.4634	0.9858	0.9810	0.9759	0.9632	0.9552	0.8398
2B	9.5333	8.6309	8.1139	7.2701	6.8772	4.0989	0.9254	0.9366	0.9399	0.9398	0.9370	0.8432
3A	8.5415	7.6700	7.1772	6.3832	6.0177	3.5064	0.9651	0.9638	0.9609	0.9522	0.9463	0.8516
4B	9.2485	8.3677	7.8634	7.0409	6.6582	3.9572	0.9456	0.9492	0.9475	0.9380	0.9302	0.7855
5B	9.5928	8.6760	8.1513	7.2960	6.8981	4.0933	0.9229	0.9211	0.9155	0.8983	0.8863	0.6942
6B	18.7810	17.0020	15.9830	14.3200	13.5450	8.0673	0.9208	0.9324	0.9356	0.9344	0.9307	0.8202
7B	10.6390	9.6386	9.0649	8.1280	7.6914	4.5985	0.9240	0.9442	0.9530	0.9620	0.9637	0.9053
8B	4.6471	4.2168	3.9697	3.5653	3.3765	2.0326	0.8948	0.9217	0.9357	0.9559	0.9640	0.9838
9B	7.0918	6.4169	6.0305	5.4003	5.1070	3.0363	0.8512	0.8559	0.8550	0.8470	0.8400	0.7043
10A	7.4956	6.7306	6.2981	5.6012	5.2804	3.0768	0.9866	0.9848	0.9816	0.9723	0.9661	0.8682
11A	12.2530	11.0100	10.3070	9.1725	8.6500	5.0529	0.9648	0.9725	0.9752	0.9761	0.9749	0.9204
13A	16.0940	14.4800	13.5650	12.0890	11.4080	6.7025	0.9013	0.9218	0.9326	0.9483	0.9547	0.9741
Mean							0.9340	0.9420	0.9445	0.9430	0.9401	0.8550
σ							0.0307	0.0254	0.0235	0.02430	0.0271	0.0687

[Notes] σ is the Standard deviation of R^2 .

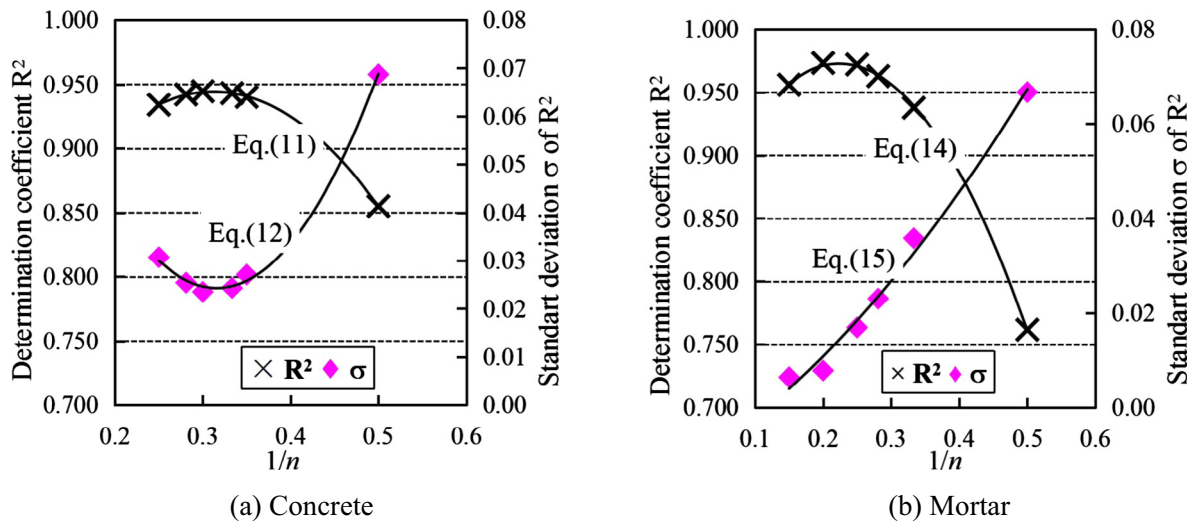


Fig. 8. The changes of R^2 and σ with $1/n$ of concrete (a) and mortar (b).

Based on the above theoretical analysis and the discussion on the experimental results, in case of FA&BFS-based GP concrete, as an universal model, we proposed to use the root function shown in Eq. (13) to describe the carbonation progress with time.

$$x = at^{0.31} \quad (13)$$

The n value of Eq. (13) is different from the theoretical result shown in Eq. (9). This is because the theoretical analysis was conducted on basis of several suppositions and there are errors in the experiment. However, the n values in Eqs. (9) and (13) are very close. This means that the results of theoretical analysis and experimental discussion are reliable.

On the other hand, toward the experimental results of FA&BFS-based GP mortar shown in Fig. 6, we also conducted the regression analysis on the relationship between carbonation depth and time, using 6 kinds of root functions (see Eq. (10), $1/n = 0.15, 0.20, 0.25, 0.28, 0.33, 0.50$). The proportional coefficient (a), i.e. carbonation rate coefficient and determination coefficient (R^2) were obtained, as shown in Table 7.

Except the square root function ($1/n = 0.50$), almost all the determination coefficients (R^2) of other regressive root functions are more than 0.90. That is to say, the root functions of $1/n = 0.15 \sim 1/3$ can nearly describe the experimental relationship

between carbonation depth and time. For determining an optimum value of $1/n$ for GP mortar, the relationship between the determination coefficient (R^2), the standard deviation (σ) and $1/n$ were plotted, as shown in the Fig. 8(b). Like as GP concrete, the R^2 increases with increasing the $1/n$, but beyond a certain $1/n$ value, the R^2 starts to decrease with the $1/n$. However, the standard deviation (σ) of R^2 increases with the $1/n$. The regressive curve equation of R^2 , $\sigma \sim 1/n$ relationship were gotten, as shown in Eqs. (14) and (15).

$$R^2 = -2.7664(1/n)^2 + 1.2372(1/n) + 0.8342, \text{ Determination coefficient : } 0.9996 \quad (14)$$

$$\sigma = 0.1466(1/n)^2 + 0.0858(1/n) - 0.0122, \text{ Determination coefficient : } 0.9892 \quad (15)$$

Through a maximum-minimum problem analysis of Eq. (14), we found that in case of GP mortar, for achieving a maximum R^2 , $1/n$ should be 0.224. And when $1/n$ is equal to 0.224, According to Eq. (15) the σ is 0.0078, which is small enough. Hence, we proposed to use the root function shown in Eq. (16) to describe the relationship between carbonation depth and elapsed time in case of FA&BFS-based GP mortar.

Table 7

The carbonation rate coefficient of FA&BFS-based GP mortar.

No.	Carbonation rate coefficient <i>a</i>						Determination coefficient R ²					
	1/ <i>n</i>						1/ <i>n</i>					
	0.15	0.20	1/4	0.28	1/3	1/2	0.15	0.20	1/4	0.28	1/3	1/2
1	5.4330	4.7253	4.0866	3.7249	3.1719	1.8457	0.9457	0.9712	0.9784	0.9744	0.9744	0.8081
4	9.2604	8.0541	6.9653	6.3486	5.4060	3.1448	0.9561	0.9817	0.9887	0.9845	0.9641	0.8136
5	2.7077	2.3523	2.0319	1.8507	1.5739	0.9118	0.9498	0.9648	0.9606	0.9492	0.9164	0.7258
7	6.0708	5.2783	4.5639	4.1597	3.5422	2.0624	0.9531	0.9760	0.9814	0.9767	0.9564	0.8123
8	6.0381	5.2498	4.5390	4.1367	3.5222	2.0495	0.9624	0.9852	0.9901	0.9848	0.9632	0.8125
9	5.3890	4.6706	4.0258	3.6620	3.1082	1.7916	0.9685	0.9601	0.9328	0.9073	0.8515	0.5972
Mean							0.9559	0.9732	0.9720	0.9628	0.9377	0.7616
σ							0.0064	0.0078	0.0169	0.0230	0.0358	0.0667

[Notes] σ is the Standard deviation of R².

$$x = at^{0.22} \tag{16}$$

4. Influencing factors of carbonation rate

In order to investigate influencing factors of the carbonation resistance of GP concrete, it is usual to use the experimental results of GP concrete specimens. The root functions used to describe exactly the carbonation rate of GP concrete and mortar are different, as shown in Eqs. (13) and (16). However, it is considered that the carbonation resistance of GP concrete is greatly dependent on that of GP matrix mortar. It is possible to use GP mortar specimens instead of GP concrete to discuss the influencing factors, excluding aggregate type and content, through comparing the carbonation rate coefficient *a* of GP mortar.

Due to the coarse aggregate particles' existence, the pink area boundary on the GP concrete's section is a jagged line rather than a circle. The jagged pink area boundary reduces the accuracy of carbonation depth's measurement. For easily guaranteeing the accuracy of carbonation test and reducing experimental works, GP mortar specimens were used for the investigation of some of influencing factors, including curing temperature, BFS fineness, alkali activator sort, and addition of retarder. It should be noted that when investigating a certain influencing factor, we compared the carbonation rate coefficient (*a*) of the same kind of GP material (mortar or concrete) with different recipes. That is to say, we did not confuse the "a" of mortar and concrete to do the factor analysis. The carbonation rate coefficients of concrete and mortar were gotten according to Eqs. (13), and (16), respectively.

4.1. Addition of retarder

Fig. 9 demonstrates the carbonation rate coefficients (*a*) of GP concrete and GP mortar with or without adding the retarder. In case of adding the retarder, the dosage was 5% of active fillers by mass. From this figure, it can be found that whether the GP concrete or the GP mortar specimen adding 5% retarder had a smaller carbonation rate coefficient, compared to the specimens without adding the retarder. At present, the reason is not clear. The retarder prolongs the setting time of GP through slowing down the dissolution of Ca²⁺ from BFS so that the GP structure forms slowly but densely [19]. Dense GP structure may be of benefit to the improvement of the carbonation resistance of GP concrete.

4.2. WG to AS ratio

Fig. 10 shows the change of the *a* value of GP concrete with WG/AS ratio by volume. It clearly shows that as the volume ratio of water glass solution to alkali activator solution increased from 0 to 1.0, the carbonation rate coefficients (*a*) increased greatly. That

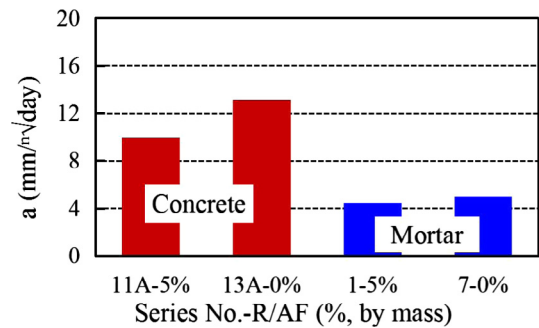


Fig. 9. Effect of retarder on the *a* value of GP concrete and mortar.

is to say, the more the water glass (WG) in the WG-NaOH solution (AS), the lower the carbonation resistance of FA&BFS-based GP concrete.

Although the GP concrete specimen using NaOH solution as alkali activator showed a better carbonation resistance than the specimens using a combination of NaOH and water glass, the compressive strength of the former at 28 days age was smaller than that of the latter when cured at room temperature [18]. Criado, et al. and Pinto, et al. [29] also reported the similar results that using the alkaline activator containing water glass causes a higher mechanical strength. Criado et al. explained the reason to be that water glass favors the polymerization process to lead to the reaction products with more Si.

4.3. AS to AF ratio and AS content

The relationship between the *a* values of FA&BFS-based GP concrete and AS/AF ratio is shown in Fig. 11. The carbonation rate coefficient of GP concrete increased with the AS/AF ratio. This result is the similar to OPC concrete. OPC concrete's carbonation resistance

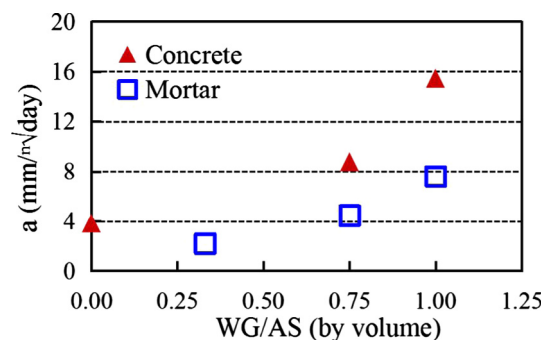


Fig. 10. The *a*-WG/AS ratio relationship of GP concrete and mortar.

generally decreases with the increase of water-cement ratio. The increase of AS/AF ratio causes the increases of Na/Si ratio and the W/AF ratio. Much water would yield more pores in hardened GP concrete. That is to say, W/AF ratio affects the carbonation resistance of GP concrete. P. Nath [14] also stated that the W/AF ratio affects the strength of GP concrete. As explained in Chapter 5, the greater the strength of GP concrete, the higher its carbonation resistance.

However, from Fig. 12, we didn't find the effect of AS content on the carbonation resistance of GP concrete.

4.4. BFS to AF ratio

The a values of GP concretes, blended with 20%, 30%, 40% and 50% BFS by mass respectively, are shown in Fig. 13. In this figure, the a values corresponding to 30% BFS were gotten by different specimens produced in June and October 2016, respectively. Though the data varies widely, it can be found that the a value decreased with increasing the ratio of BFS to the active filler (AF), i.e. the carbonation resistance of FA&BFS-based GP concrete becomes high as the BFS content increases. This attributes to that the increase of BFS content improves the compressive strength of the FA&BFS-based GP concrete that becomes more compact [17]. However, we also found that the relationship between the a value and the BFS/AF ratio is not proportional, with the increase of BFS/AF ratio, especially over 40% the decrease of the a value became small.

It should be noted that we also tried to investigate the carbonation resistance of GP concrete without mixing BFS in this study. But because the boundary of pink color area was so vague that the carbonation depth couldn't be measured properly (see Series No.12B in Table 5), we have to give up this discussion here.

4.5. BFS fineness

The BFS with Blaine fineness of 3000, 4000, and 6000 cm^2/g were used to investigate the effect of BFS fineness on the carbonation resistance of FA&BFS-based GP concrete. Obtained results are shown in Fig. 14. The carbonation rate coefficient a of the GP concrete using the BFS with 3000 cm^2/g of Blaine fineness was the largest. But the a values of the GP concretes using BFS 40P and BFS 60P were almost the same. Therefore, we can say that when the fineness of BFS reaches a certain level, e.g. 4000 cm^2/g in this study, its effect on the carbonation resistance of FA&BFS-based GP concrete becomes unobvious.

From the viewpoint of strength, Talling, et al. [30] pointed out that the optimum Blaine fineness of slag is 4000 cm^2/g , and Wang et al. [31] stated that the optimum Blaine fineness of slag depends on the type of slag and varies between 4000 and 5500 cm^2/g . If referring to the results shown in the Chapter 5 that the carbonation

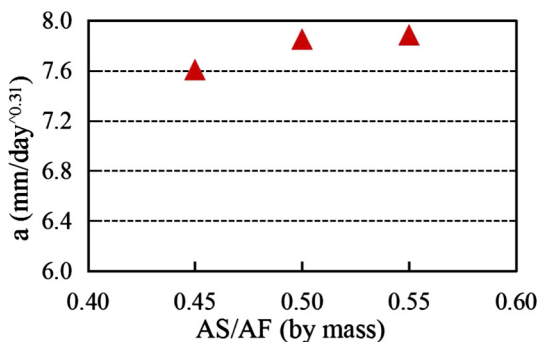


Fig. 11. The a -AS/F ratio relationship of GP concrete.

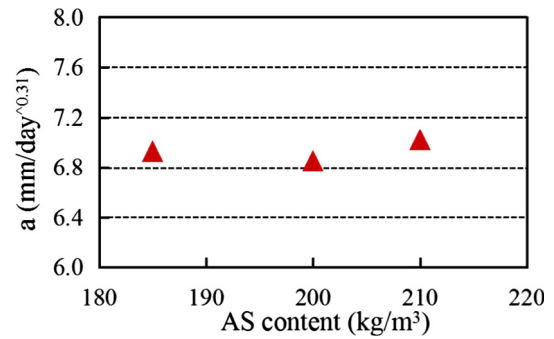


Fig. 12. The a -AS content relationship of GP concrete.

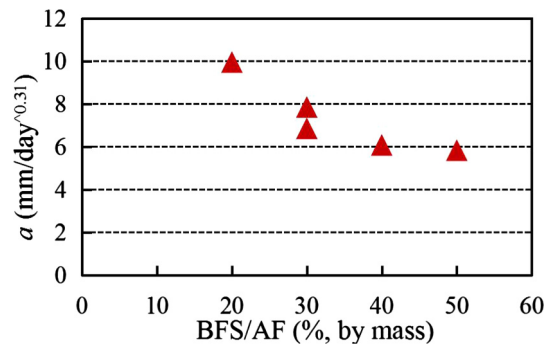


Fig. 13. The a -BFS/F ratio relationship of GP concrete.

resistance of GP concrete correlates closely with its strength, the results shown in Fig. 14 are reasonable.

4.6. Curing temperature

Since the best $1/n$ values of the root functions for GP mortar cured at ambient temperature and high temperatures are different, as shown in Table 7 (see Series No.1–3). Hence, instead of carbonation rate coefficient, we directly compared the carbonation depths at the same carbonation time for different curing temperatures, as shown in Fig. 15. It can be clearly found that GP mortars cured at 60 °C and 80 °C had almost the same carbonation depth, but 20 °C curing yielded about 3 times carbonation depth of heat curing. That is to say, heat curing can improve the carbonation resistance of FA&BFS-based GP concrete.

4.7. Na to Si ratio

Fig. 16 shows the influence of Na/Si ratio by molar on the carbonation resistance of FA&BFS-based GP concrete with 0.50 of

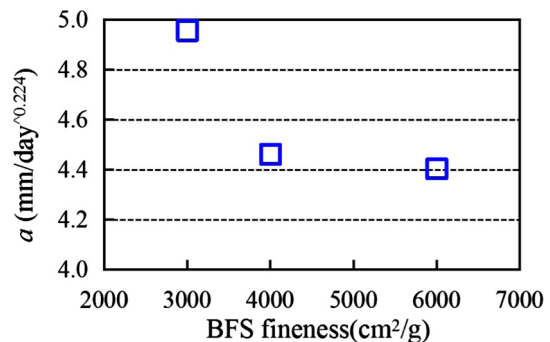


Fig. 14. The effect of BFS fineness on the a value of GP mortar.

AS/AF ratio. The larger Na/Si ratio, the smaller the a value. The relationship between the a value and Na/Si ratio can be roughly described by a power function.

5. Relationship between compressive strength and carbonation resistance

The relationship between the 28-days compressive strength and the carbonation rate coefficient (a) are shown in Fig. 17 for 13 series of GP concrete, which were cured in the 20 °C air. Though the a values dropped as the compressive strength increased on the whole, they ranged widely even for the same compressive strength. This is because although the compressive strength depends on the denseness degree of concrete, the carbonation resistance of GP concrete is affected by not only the denseness degree, but also the sort of alkali activator, and pore characteristics, etc. For example, even if the pores' amount and size distribution are the same, the concrete with the pores that are connected with the outside would have a low carbonation resistance.

6. Conclusions

In order to clarify the carbonation resistance of FA&BFS-based GP concrete, in this study the accelerated carbonation tests of GP concrete and GP mortar were performed. The carbonation depth was measured within 5 min later after spraying phenolphthalein solution. The relationship between the carbonation depth and time was further examined based on the experimental results and by theoretical analysis. Finally, we discussed the influencing factors of the carbonation resistance of FA&BFS-based GP concrete in detail through comparing the carbonation rate coefficients of different specimens. Main conclusions are as follows.

- (1) The relationship between carbonation depth and elapsed time of FA&BFS-based GP concrete and GP mortar, which are cured in the ambient air, can be expressed by root functions, shown in Eqs. (13) and (16) where $1/n$ values are 0.31, and 0.22 respectively. The increasing rate of carbonation depth of FA&BFS-based GP concrete in the early time is larger than that of OPC concrete.
- (2) As the effects of raw materials on the carbonation resistance of FA&BFS-based GP concrete, the addition of the retarder mainly composed of potassium sodium tartrate can improve the carbonation resistance of FA&BFS-based GP concrete cured in the ambient air. The finer the BFS, the smaller the carbonation rate coefficient (a) of FA&BFS-based GP concrete. However, the decrease of a value with the increase of BFS fineness becomes smaller and smaller when the Blaine fineness of BFS is larger than 4000 g/cm².

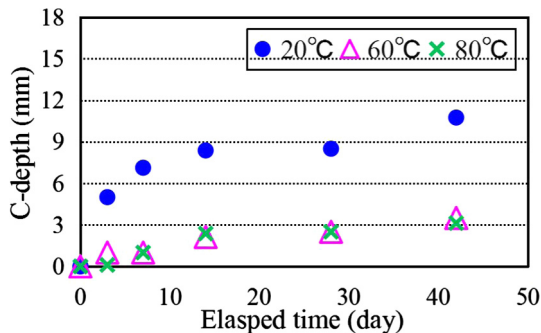


Fig. 15. The effect of curing temperature on the carbonation resistance of GP mortar.

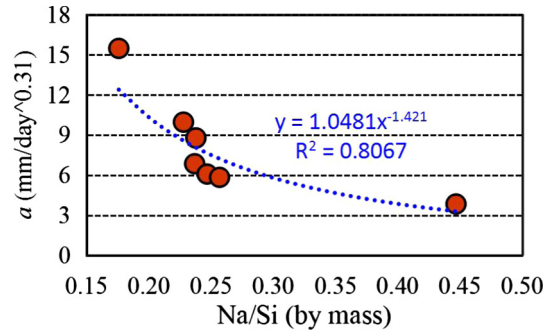


Fig. 16. The change of the a value of GP concrete with Na/Si ratio.

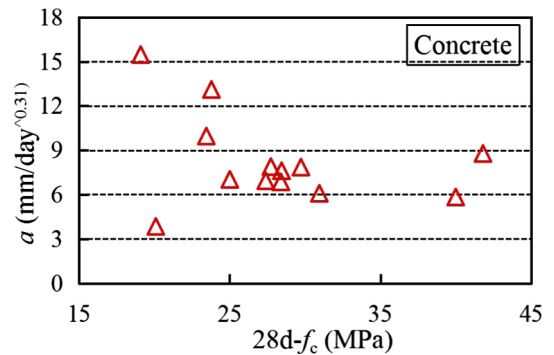


Fig. 17. Relationship between the a value and compressive strength.

- (3) As the effects of mix proportions on the carbonation resistance of FA&BFS-based GP concrete, with the increase of BFS ratio in active fillers (AF), the carbonation rate coefficient of FA&BFS-based GP concrete decreases. However, the decrease becomes small when the BFS ratio is above 40%. The higher the NaOH content in the alkaline activator (AS) composed of sodium silicate and NaOH, the higher the carbonation resistance. The compressive strength of FA&BFS-based GP concrete only using sodium hydroxide is, however, lower than that using sodium silicate and NaOH together. Also, with increasing the AS/AF ratio or Water-FA ratio, the carbonation rate coefficient increases. However, the effect of AS content was not clearly found from the experimental results. Moreover, for the same AS/AF ratio, the carbonation rate coefficient declines with the increase of Na/Si ratio.
- (4) Curing temperature greatly influences the properties of FA&BFS-based GP concrete. Curing at room temperature yields a lower carbonation resistance, compared to heat curing. There is, however, no great difference between 60°C and 80 °C curing, if the curing duration is the same.
- (5) The carbonation resistance of GP concrete is related to its compressive strength. The concrete having a higher strength generally tends to have a higher carbonation resistance. But the carbonation resistance of GP concrete is also affected by other factors, such as alkaline activator type. The experimental results in this study showed that the carbonation rate coefficient of FA&BFS-based GP concrete doesn't always decrease with its compressive strength, as shown in Fig. 17.

Acknowledgements

The authors would like to thank H. Takagaito and T. Nagai in Mie Prefecture Testing Center for Construction Materials, and S.

Hashizume and T. Okada in Toho Chemical Industry Co., Ltd for their assistance in the production of the concrete specimens. We also deeply appreciate Y. Tanigawa, an emeritus professor at Nagoya University, for his valuable advice.

References

- [1] D.N. Huntzinger, T.D. Eatmon, A life-cycle assessment of Portland cement manufacturing: comparing the traditional process with alternative technologies, *J. Cleaner Prod.* 17 (7) (2009) 668–675.
- [2] C. Meyer, The greening of the concrete industry, *Cem. Concr. Compos.* 31 (8) (2009) 601–605.
- [3] J. Davidovits, Geopolymers of the first generation: silface-process, in: *Geopolymer'88: First European Conference on Soft Mineralogy*, Compiègne, France 2 (1988) 49–67.
- [4] D.A. Crozier, J.G. Sanjayan, Chemical and physical degradation of concrete at elevated temperatures, *Concr. Australia* 25 (1) (1999) 18–20.
- [5] S. Thokchom, P. Ghosh, S. Ghosh, Performance of fly ash based geopolymer mortars in sulphate solution, *J. Eng. Technol. Rev.* 3 (1) (2010) 36–40.
- [6] B.V. Rangan, Geopolymer concrete for environmental protection, *Indian Concr. J.* 88 (4) (2014) 41–59.
- [7] Z. Li, Z. Ding, Y. Zhang, Development of sustainable cementitious materials, in: *International Workshop on Sustainable Development and Concrete Technology* (2004) 55–76.
- [8] P. Duxson, J.L. Provis, G.C. Lukey, J.S.J. van Deventer, The role of inorganic polymer technology in the development of green concrete, *Cem. Concr. Res.* 37 (12) (2007) 1590–1597.
- [9] A.A. Adam, Strength and durability properties of alkali activated slag and fly ash-Based geopolymer concrete, RMIT University Melbourne, Australia, 2009, pp. 79–89.
- [10] D.W. Law, A.A. Adam, T.K. Molyneux, I. Patnaikuni, A. Wardhono, Long term durability properties of class F fly ash geopolymer concrete, *Mater. Struct.* 48 (3) (2015) 721–731.
- [11] J. Davidovits, Geopolymer, Green Chemistry and Sustainable Development Solutions: Proceedings of the World Congress Geopolymer 2005, Geopolymer Institute (2005) 9–15.
- [12] K.I. Song, J.K. Song, B.Y. Lee, K.H. Yang, Carbonation characteristics of alkali-activated blast-furnace slag mortar, *Adv. Mater. Sci. Eng.* (2014) 1–11.
- [13] S.A. Bernal, J.L. Provis, B. Walkley, R. San Nicolas, J.D. Gehman, D.G. Brice, et al., Gel nanostructure in alkali-activated binders based on slag and fly ash, and effects of accelerated carbonation, *Cem. Concr. Res.* 53 (2013) 127–144.
- [14] M. Criado, A. Palomo, A. Fernández-Jiménez, Alkali activation of fly ashes. Part 1: effect of curing conditions on the carbonation of the reaction products, *Fuel* 84 (16) (2005) 2048–2054.
- [15] K. Pasupathy, M. Berndt, A. Castel, J. Sanjayan, R. Pathmanathan, Carbonation of a blended slag-fly ash geopolymer concrete in field conditions after 8 Years, *Constr. Build. Mater.* 125 (2016) 661–669.
- [16] S. Sundar Kumar, J. Vasugi, P.S. Ambily, B.H. Bharatkumar, Development and determination of mechanical properties of fly ash and slag blended geopolymer concrete, *Int. J. Sci. Eng. Res.* 4 (8) (2013).
- [17] P. Nath, P.K. Sarker, Effect of GGBFS on setting, workability and early strength properties of fly ash geopolymer concrete cured in ambient condition, *Constr. Build. Mater.* 66 (2014) 163–171.
- [18] T. Nagai, Z. Li, H. Takagaito, A. Suga, Experimental study on the mechanical properties of geopolymer concrete using fly ash and ground granulated blast furnace slag, *Proc. Jpn. Concr. Inst.* 39 (1) (2017) 2077–2082.
- [19] T. Okada, Z. Li, S. Hashizume, T. Nagai, Experimental study on the properties of fly ash and ground granulated blast furnace slag based geopolymer concrete using retarder, *Proc. Jpn. Concr. Inst.* 38 (1) (2016) 2295–2300.
- [20] M. Criado, W. Aperador, I. Sobrados, Microstructural and mechanical properties of alkali activated Colombian raw materials, *Materials* 9 (3) (2016) 158.
- [21] K. Harada, I. Ichimiya, S. Tsugo, K. Ikeda, Fundamental study on the durability of geopolymer mortar, *Proc. Jpn. Concr. Inst.* 33 (1) (2011) 1937–1942.
- [22] M.S. Badar, K. Kupwade-Patil, S.A. Bernal, J.L. Provis, E.N. Allouche, Corrosion of steel bars induced by accelerated carbonation in low and high calcium fly ash geopolymer concretes, *Constr. Build. Mater.* 61 (2014) 79–89.
- [23] E. Vesikari, Carbonation and chloride penetration in concrete with special objective of service life modelling by the factor approach, *Research Report* (2009) 4–6.
- [24] T. Sasaki, I. Shimabukuro, H. Oshita, Analytical study on prediction of pore volume changes due to carbonation of concrete based on detailed carbonation model introduced chemical equilibrium theory, *J. Jpn. Soc. Civ. Eng. E* 62 (3) (2006) 555–568.
- [25] T. Ishida, K. Maekawa, Modeling of pH profile in pore water based on mass transport and chemical equilibrium theory, *J. Jpn. Soc. Civ. Eng.* 47 (648) (2000) 203–215.
- [26] K.H. Yang, E.A. Seo, S.H. Tae, Carbonation and CO₂ uptake of concrete, *Environ. Impact Assess. Rev.* 46 (2014) 43–52.
- [27] L. Czarnecki, P. Woyciechowski, Modelling of concrete carbonation; is it a process unlimited in time and restricted in space?, *Bull. Polish Acad. Sci. Techn. Sci.* 63 (1) (2015) 43–54.
- [28] S. Li, Z. Li, T. Nagai, T. Okata, Neutralization resistance of fly ash and blast furnace slag based geopolymer concrete, *Proc. Jpn. Concr. Inst.* 39 (1) (2017) 2023–2028.
- [29] A.T. Pinto, Alkali-activated metakaolin based binders, PhD Thesis, University of Minho (2004).
- [30] B. Talling, J. Brandstetr, Present state and future of alkali-activated slag concretes, in: *Proceedings of 3rd International Conference on Fly Ash, Silica Fume, Slag And Natural Pozzolans In Concrete*, Trondheim Norway (1989) 1519–1546.
- [31] S.D. Wang, K. Scrivener, P. Pratt, Factors affecting the strength of alkali-activated slag, *Cem. Concr. Res.* 24 (1994) 1033–1043.